

The shelf life of wine

Geoff Mercer

University of New South Wales @ADFA

Andy Wilkins

CSIRO

Jonathon Crook

Victoria University of Wellington

Steve Barry

University of New South Wales @ADFA

Andrew Fowler

University of Limerick

1 Introduction

The aim of this project was to investigate and develop models for the shelf life of bottled wine and, in particular, the effects of elevated temperatures on the aging process. The MISG group divided the problem into three sub-problems. First, calculations were made to describe the temperature of wine in a single bottle when subjected to an elevated external temperature and then this was extended to pallets of cartons of wine. This has application to determining the temperature of the wine during both the transport and storage of wine. Second, equations were derived for the gas flow through the cork when a wine bottle is subject to oscillatory temperature variation such as is common in a domestic storage situation. This has important implications to the aging processes in the wine as cork breathing can lead to increased oxidation of the wine. Third, the temperature dependent reaction rates of the wine aging processes were considered and calculations performed on how elevated temperatures decrease the shelf life compared to ideal cellaring conditions. Suggestions were made as to relatively simple experiments that can be performed to test the aging models developed here.

2 Heating of the bottle and wine

The temperature of wine in a bottle is quantified using numerical simulation for two simple cases: an initially cool bottle standing in a hot environment; an initially cool, large pallet of bottles standing in a hot environment. These are the two extremes which can occur during the transportation and storage of wine. Throughout the numerical simulations the physical parameters used are given in Tables 1 and 2. The numerical simulations are performed using a finite element package FlexPDE that is space and time adaptive to enable the fine spatial structure such as the glass and cork to be modelled.

Feature	value
Bottle base radius	3.81 cm
Bottle neck radius	1.48 cm
Bottle base height	20.0 cm
Bottle neck height	10.0 cm
Total bottle height	30.0 cm
Cork height	4.0 cm
Bottle volume	981 ml
Wine volume	750 ml
Cork volume	13 ml
Glass volume	213 ml
Head-space volume	5 ml
Volume occupied by bottle in carton	1920 ml
Glass thickness	0.47 cm

Table 1: Values of the parameters used in this study.

Material	k	c	ρ	κ ($\text{m}^2 \text{s}^{-1}$)	κ ($\text{cm}^2 \text{hr}^{-1}$)
Wine	0.52	4180	1000	0.083×10^{-6}	4.48
Glass	1.0	550	2500	0.727×10^{-6}	26
Air	0.016	1000	1.20	13.3×10^{-6}	480
Cork	0.04	800	250	0.20×10^{-6}	7.2
Paper	0.18	1400	1000	0.071×10^{-6}	2.6

Table 2: Thermal properties of relevant materials. Thermal conductivity k ($\text{W m}^{-1} \text{K}^{-1}$), heat capacity c ($\text{J kg}^{-1} \text{K}^{-1}$), density ρ (kg m^{-3}), diffusivity $\kappa = k/(\rho c)$ in $\text{m}^2 \text{s}^{-1}$ and $\text{cm}^2 \text{hr}^{-1}$.

2.1 Heat conduction through a single wine bottle

2.1.1 Numerical simulation

Consider the conduction of heat through a single bottle of wine when subjected to an elevated temperature. Of interest is the time scale involved for the increase in temperature of the wine. We will consider one typical example where the wine, bottle, air and cork are initially at 10°C . At time $t = 0$ the air surrounding the bottle is raised to 40°C and held constant throughout the simulation. Heat is conducted through the wine, bottle, headspace air and cork. To simplify the calculations convection is ignored. Mathematically we have

$$\nabla \cdot (k \nabla T) = \rho c \frac{\partial T}{\partial t} \text{ with } T(r, z, t = 0) = 10^\circ\text{C} \text{ and } T(r = \text{exterior}, z, t) = 40^\circ\text{C}. \quad (1)$$

Here r and z are the radial and axial coordinates respectively, ∇ is the spatial derivative operator in the appropriate coordinates, t is time, k is the thermal conductivity, ρ the density and c the specific heat capacity. The latter 3 parameters vary with r and z , and their values in the wine, glass, cork and air are given in Table 2. Much of this data is found in [3]. There is nothing special about the values 10°C and 40°C , the results hold generally and these values are used for indicative purposes. The paper label on the wine bottle is ignored as its effect

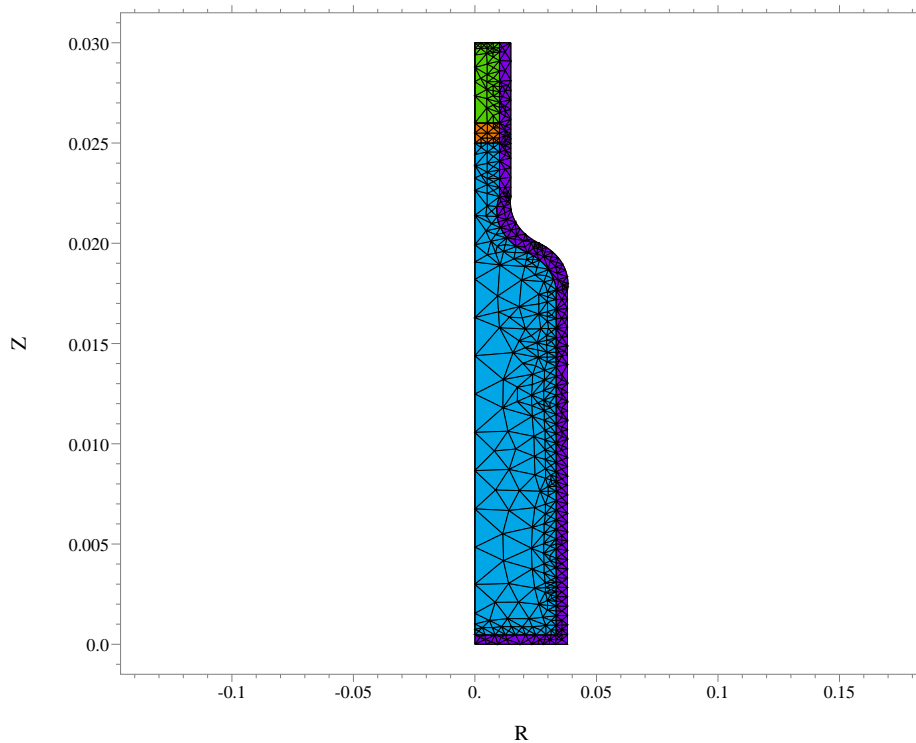


Figure 1: A section of the 3D wine bottle showing the mesh used for the finite element simulation.

on the heat transfer is negligible compared to the glass and wine component. A Dirichlet boundary condition at the air-glass interface is used. This is an extreme case resulting in the fastest heating of the wine and so any estimates obtained for heating times will be on the pessimistic side.

Figure 1 shows a section view of the 3D wine bottle and the finite element mesh used in the simulation. More mesh points are used in areas of large gradients such as through the glass to ensure accuracy of the solution.

Figure 2 shows the pattern of heat conduction through the system with a snapshot of temperature at time 10 minutes as a contour plot. At this stage the glass and the wine in the bottle's neck is close to 40°C , the exterior of the wine is around 35°C and the central area around 11°C . Figure 3 records temperature as a function of time at various positions in the bottle. It is clear from the simulation that the wine in the neck approaches the external ambient temperatures within approximately 1000 seconds (16 minutes), while the temperature in the bottle's middle takes approximately 7000 seconds (2 hours) to almost equilibrate with the ambient.

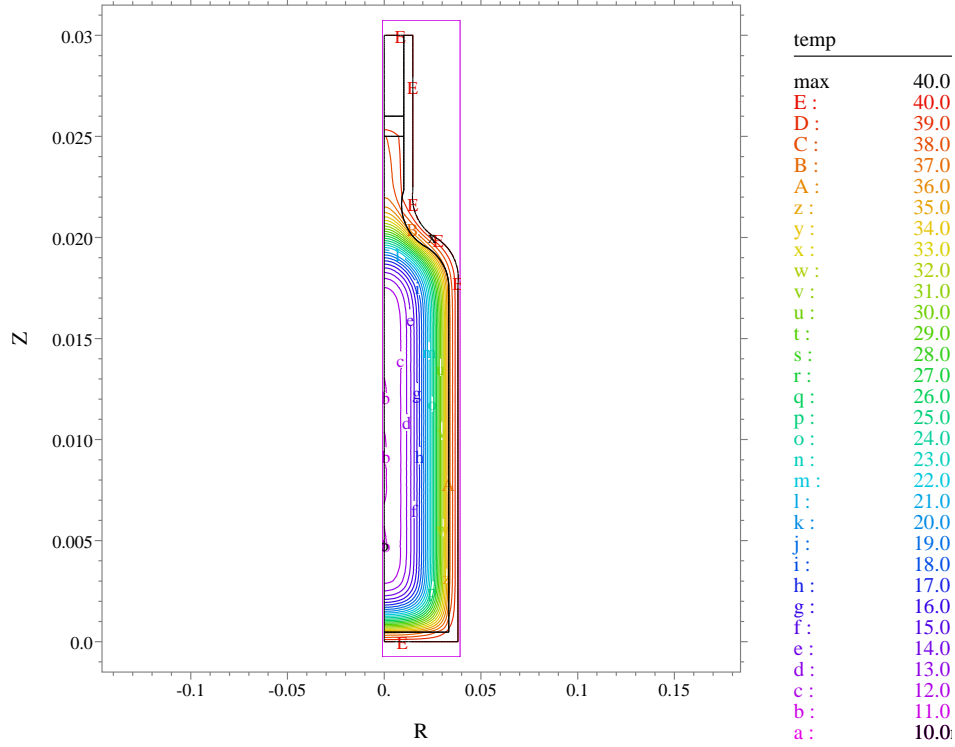


Figure 2: A snapshot of the temperature profile of the wine bottle section after 10 minutes of heating.

2.1.2 Simplified approach

It is possible, using simplifying assumptions, to get a general guide to the time scales involved. For heat conduction problems there is the approximate relationship

$$\text{time taken to travel distance} \sim \frac{\text{distance}^2}{4\kappa}, \quad (2)$$

where κ is the diffusivity ($\kappa = k/(\rho c)$). Hence, for a distance of 3.81 cm (the radius of the bottle) and $\kappa = 4.48 \text{ cm}^2 \text{ hr}^{-1}$ (diffusivity of wine), this yields a time scale of approximately 0.8 hours (2900 seconds) which is consistent with the results presented in Figure 3.

As another approximation consider a well mixed bottle of wine so that the average temperature is the quantity of interest. The average temperature in the wine as a function of time is

$$T_{\text{av}}(t) = \frac{1}{\text{Volume of wine}} \int_{\text{wine}} T(r, z, t) dV.$$

Suppose the average temperature obeys Newton's law of cooling (or heating)

$$\frac{dT_{\text{av}}}{dt} = h(T_{\text{air}} - T_{\text{av}}), \quad (3)$$

for some effective heat transfer coefficient h that needs to be determined. Solving equation (3) gives

$$T_{\text{av}}(t) = T_{\text{air}} + (T_{\text{initial}} - T_{\text{air}})e^{-ht}. \quad (4)$$

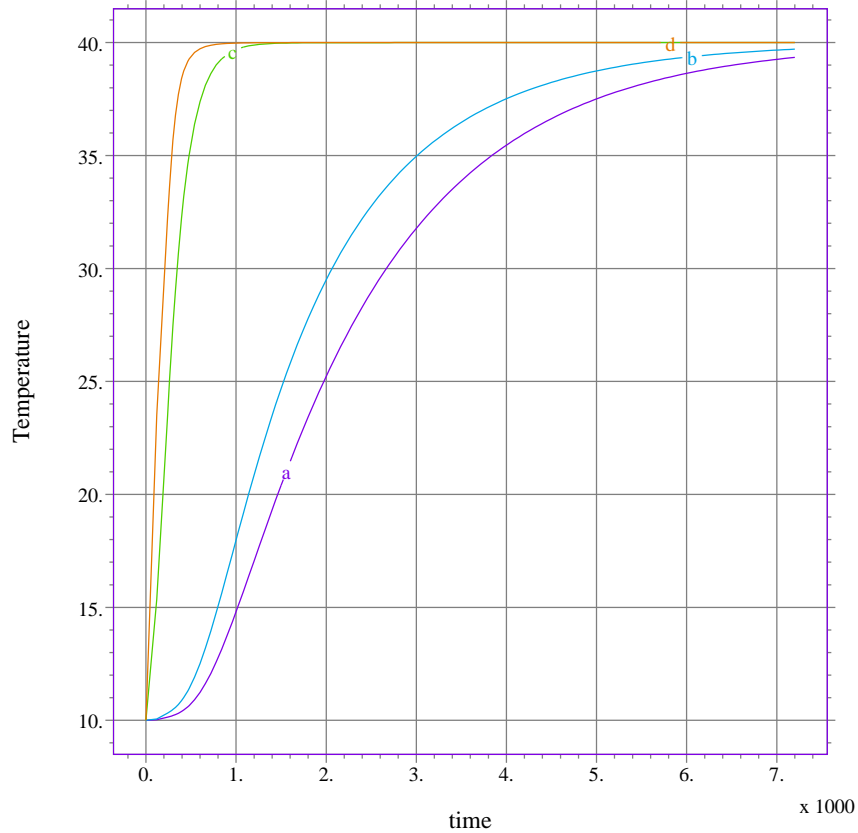


Figure 3: Temperature as a function of time at various places in the bottle for 2 hours (7200 s) of heating. (a) wine in the bottle's centre near the bottle's base; (b) wine in the bottle's centre near the bottle's top; (c) top of the wine; (d) air at the base of the cork.

Rearranging gives

$$-ht = \log((T_{av} - T_{air}) / (T_{initial} - T_{air})) . \quad (5)$$

To verify if investigating the average temperature is a reasonable assumption for our numerical solution we calculate the average temperature of the wine in the bottle from the numerical simulation results and test equation (5). Figure 4 is a plot of equation (5). A straight line plot means we have a good approximation. In the figure the data does indeed fit a straight line after approximately 1000 seconds. The slope of the line is approximately $h = 6.4 \times 10^{-4} \text{ s}^{-1} = 2.3 \text{ hr}^{-1}$. This has shown that the averaged Newton's law approach is suitable to the accuracy required.

In practical applications there exists other effects not considered in the idealised numerical simulation. These include: (a) convective or mechanical mixing of the wine, (b) cooling of the surrounding air by the wine, and (c) incomplete knowledge of the surrounding air temperature. It may be appropriate to use a heat transfer coefficient from the air to the bottle (instead of keeping the exterior temperature fixed), but in most practical situations it is more useful to use the simple Newton's law, detailed above, rather than a full three dimensional numerical solution.

The key parameter governing wine the temperature is the heat transfer coefficient h .

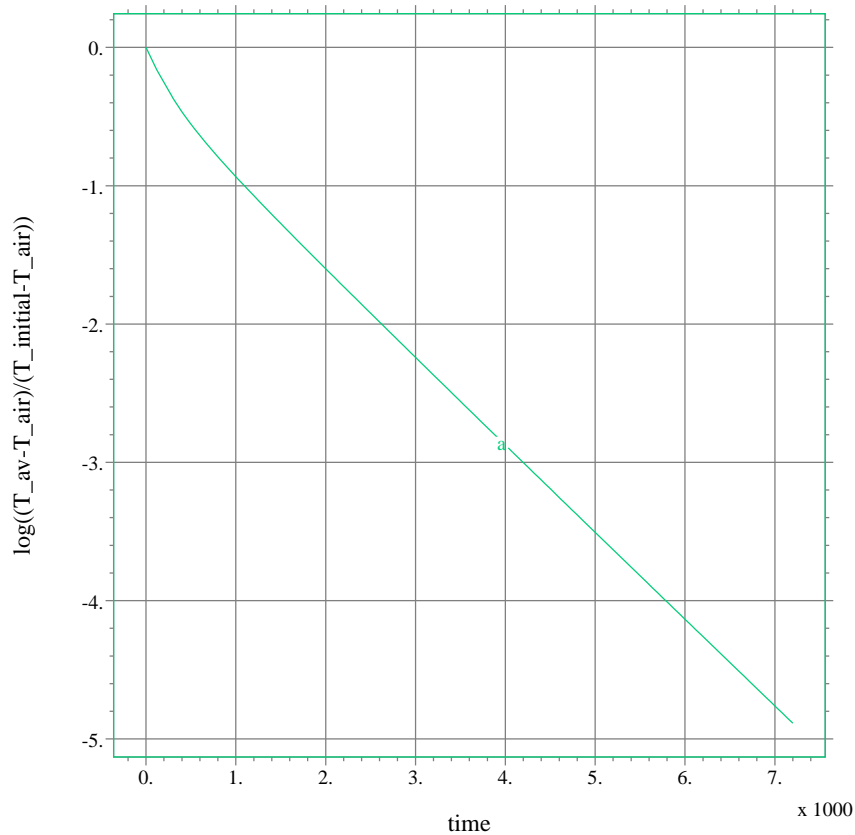


Figure 4: Plot of $\log((T_{av} - T_{air})/(T_{initial} - T_{air}))$ against t ($t = 0$ to 7200 s,) where T_{av} is the average wine temperature. The straight line has slope $6.4 \times 10^{-4} \text{ s}^{-1}$.

Here it has been ‘derived’ from a numerical simulation which represents reality reasonably accurately. In the event that a true experimentally derived value is required the following experiment could be performed. A typical bottle of wine could be placed in a heat bath and the average temperature of the wine plotted in a manner similar to Figure 3. Both the heat bath and the wine should be agitated in a way that duplicates the mixing that will be experienced in real life. The equivalent of Figure 4 yields the heat transfer coefficient h . However, given the results of the next section, it appears unlikely that such accuracy is needed.

2.2 Heat conduction through an array of bottles

2.2.1 Numerical simulation

Armed with the knowledge that it is sufficient to model bottles as averaged ‘lumps’ obeying Newton’s cooling law, it is now appropriate to study heat flow through and around an array of bottles. Numerical simulations are performed for this scenario. The simulation is run using only one row of bottles, but the boundary conditions are periodic so that the results hold for an infinite array of bottles which is more typical of a stacked container. The following assumptions are used.

1. The wine and glass are lumped together into one component with thermal properties of the wine.
2. The cardboard in the packing material is ignored: in real life it mostly serves to prevent convection and has limited thermal effect.
3. The heat transfer is assumed to be purely conductive through the air. Convection is ignored, but if present it may substantially speed heat flow through the array. In this respect the simulations are a best case scenario and in reality the heating time will be shorter due to convection effects.
4. The volume fraction of the wine and glass is 0.5 (corresponding roughly to 981 ml/1920 ml, see Table 1), and the volume fraction of the air is 0.5.

All components in the model are initially at 10°C. To simulate heating in a container or truck during transport the left-hand edge is raised to and kept constant at 40°C for times $t \geq 0$. Mathematically this is

$$\nabla \cdot (k \nabla T) = \rho c \frac{\partial T}{\partial t} \quad \text{with } T(x, y, t = 0) = 10^\circ\text{C} \quad \text{and } T(x = 0, y, t) = 40^\circ\text{C} . \quad (6)$$

Once again, there is nothing special about the values of 10°C and 40°C, the main results below are general. Figure 5 shows a snapshot of temperature at time 300 hours and Figure 6 shows temperature logs at various places in the bottle. After 300 hours the temperature in the first bottle is almost at the outer ambient temperature, the temperature in the third bottle is about 22°C and the seventh bottle is not much above the initial temperature.

2.2.2 Simplified approach

The heat transfer through the system can be well modelled by a one dimensional diffusion equation with constant effective diffusivity κ_{eff} . That is

$$\kappa_{\text{eff}} \frac{\partial^2 T}{\partial x^2} = \frac{\partial T}{\partial t} \quad \text{with } T(x, t = 0) = T_{\text{initial}} \quad \text{and } T(x = 0, t) = T_{\text{hot}} . \quad (7)$$

The effective diffusivity κ_{eff} is an averaged diffusivity and is independent of spatial position and needs to be found from experiments or numerical simulations. The solution of equation (7) is well known to be

$$T(x, t) = T_{\text{hot}} + (T_{\text{initial}} - T_{\text{hot}}) \text{erf} \left(\frac{x}{\sqrt{4\kappa_{\text{eff}}t}} \right) , \quad (8)$$

where the error function, $\text{erf}(y)$, is

$$\text{erf}(y) = \frac{2}{\sqrt{\pi}} \int_0^y e^{-z^2} dz . \quad (9)$$

It is possible to extract a value for κ_{eff} from the 2D numerical simulation. Integrals of error functions are well known and lead to

$$\begin{aligned} \int_0^\infty (T(x, t) - T_{\text{initial}}) dx &= (T_{\text{hot}} - T_{\text{initial}}) \int_0^\infty \left(1 - \text{erf} \left(\frac{x}{\sqrt{4\kappa_{\text{eff}}t}} \right) \right) dx \\ &= \sqrt{\frac{4\kappa_{\text{eff}}t}{\pi}} (T_{\text{hot}} - T_{\text{initial}}) . \end{aligned} \quad (10)$$

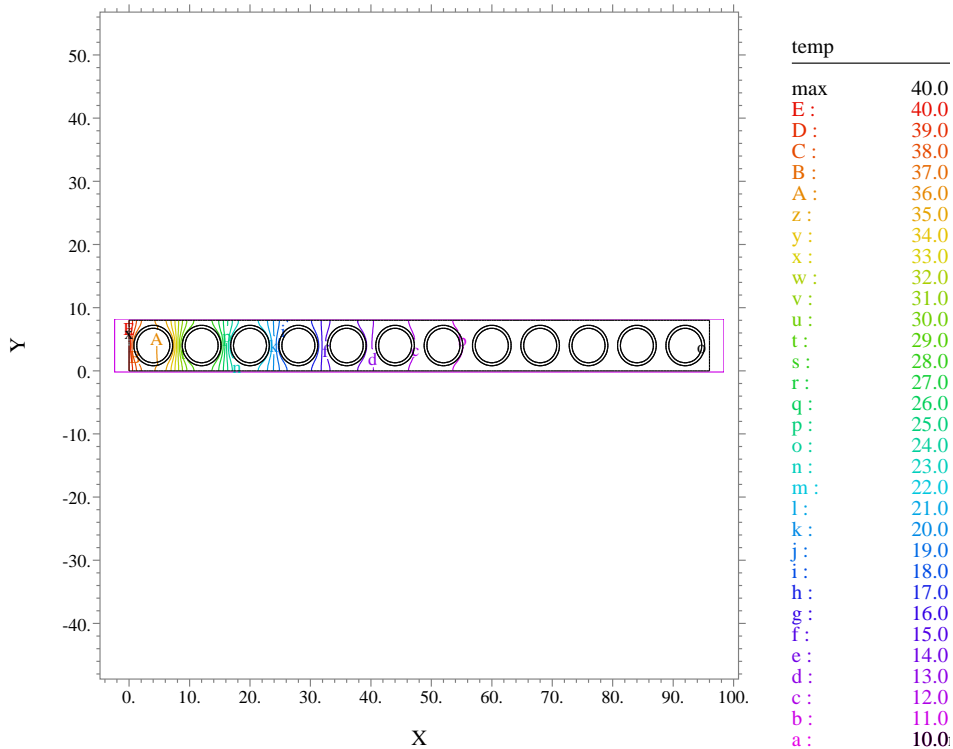


Figure 5: A snapshot of the temperature profile of the bottles and surrounding air after 300 hours of heating. The initial column of bottles (represented by the single bottle on the left) is close to ambient.

Hence, if the theory is correct, plotting the integral on the left against \sqrt{t} should yield a straight line. This is indeed true for this numerical simulation and the straight line has slope

$$\frac{4\kappa_{\text{eff}}}{\pi} = 1.27 \text{ cm}^2 \text{ hr}^{-1}, \quad \text{which implies } \kappa_{\text{eff}} \approx 1.0 \text{ cm}^2 \text{ hr}^{-1}.$$

The next subsection justifies this quantity with further theory. As has been mentioned before, this parameter dictates the distance travelled by heat through the rule-of-thumb formula equation (2). Therefore, in 1 hour heat will have diffused approximately 1 cm, and in 12 hours approximately 2.5 cm.

2.2.3 The effective diffusivity from theory

In this section the effective conductivity and heat capacity (and hence diffusivity) for the array of wine bottles packed in cartons is explored theoretically in order to check the apparently low value of κ_{eff} quoted in equation (2.2.2). Packings of both spheres and cylinders in a space are considered.

Let $\phi = \text{volume fraction of wine} = 0.5$. If the wine and air increase in temperature at the same rate, as suggested by the simulation, the effective heat capacity of the wine-air mixture is simply a weighted average

$$(\rho c)_{\text{eff}} = \phi \times (\rho c)_{\text{wine}} + (1 - \phi) \times (\rho c)_{\text{air}} \approx 2 \times 10^6 \text{ J K}^{-1} \text{ m}^{-3}. \quad (11)$$

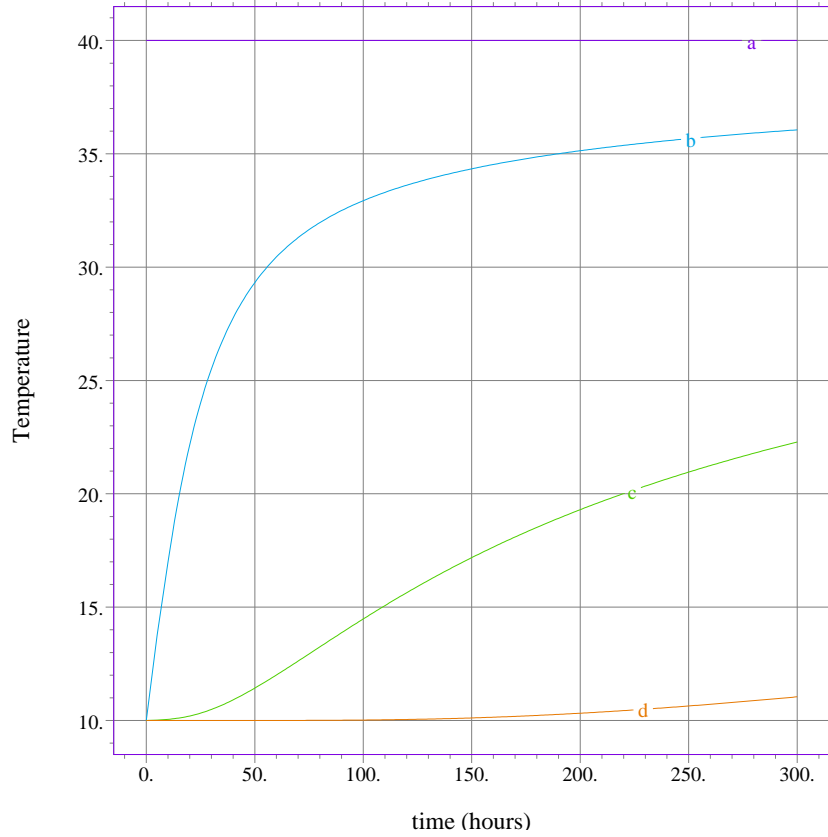


Figure 6: Temperature as a function of time (a) at the left edge; (b) in the first bottle from the left edge; (c) third bottle; (d) seventh bottle.

The literature reveals many different approximations for the effective thermal conductivity of different shapes packed in air. We will outline five of these.

Series approximation

Treating the wine and air in series (for example wine, air, wine, air, wine, ...) results in

$$k_{\text{eff}}^{\text{series}} = \phi k_{\text{wine}} + (1 - \phi) k_{\text{air}}. \quad (12)$$

This provides an upper bound on k_{eff} . Inserting parameter values yields $k_{\text{eff}}^{\text{series}} = 0.268 \text{ W m}^{-1} \text{ K}^{-1}$.

Parallel approximation

Treating the wine and air in parallel results in

$$\frac{1}{k_{\text{eff}}^{\text{parallel}}} = \frac{\phi}{k_{\text{wine}}} + \frac{1 - \phi}{k_{\text{air}}}. \quad (13)$$

This provides a lower bound on k_{eff} . Inserting parameter values yields $k_{\text{eff}}^{\text{parallel}} = 0.031 \text{ W m}^{-1} \text{ K}^{-1}$.

Maxwell approximation

[6] improved upon the lower bound given by the parallel approximation for the situation for conducting spheres of given volume fraction ϕ periodically dispersed in a insulating medium. His formula is

$$\frac{k_{\text{eff}}^{\text{m}} - k_{\text{air}}}{k_{\text{eff}}^{\text{m}} + k_{\text{air}}} = \phi \frac{k_{\text{wine}} - k_{\text{air}}}{k_{\text{wine}} + k_{\text{air}}}. \quad (14)$$

Inserting parameter values gives $k_{\text{eff}}^{\text{m}} = 0.044 \text{ W m}^{-1} \text{ K}^{-1}$.

Cheng and Torquato approximation

[2] found an approximate expression for the effective conductivity of a dilute mixture of conducting spheres as

$$k_{\text{eff}}^{\text{ct}} = k_{\text{air}} \left(1 - \frac{3\phi}{D_{\text{ct}}} \right), \text{ where } D_{\text{ct}} = -\beta_1^{-1} + \phi + c_1\beta_3\phi^{10/3} \quad (15)$$

$$+ c_2\beta_5\phi^{14/3} + c_3\beta_3^2\phi^{17/3} + c_4\beta_7\phi^6 + c_5\beta_3\beta_5\phi^7 + c_6\beta_9\phi^{22/3}, \beta_i = \frac{k_{\text{wine}} - k_{\text{air}}}{k_{\text{wine}} + (i+1)k_{\text{air}}/i} \quad (16)$$

and $c_1 = 1.30472$, $c_2 = 0.07232$, $c_3 = -0.52895$, $c_4 = 0.15256$, $c_5 = -0.30667$, $c_6 = 0.01045$. Inserting parameter values yields $k_{\text{eff}}^{\text{ct}} = 0.066 \text{ W m}^{-1} \text{ K}^{-1}$.

Perrins, McKenzie and McPhedran approximation

[9] calculated an approximation to the effective conductivity for the situation where conducting cylinders with volume fraction ϕ are immersed in an insulating medium. To low order, their expression reads

$$k_{\text{eff}}^{\text{pmm}} = k_{\text{air}} \left(1 + \frac{2\beta\phi}{1 - \beta\phi - 0.305827\beta^2\phi^4} \right). \quad (17)$$

Inserting parameter values yields $k_{\text{eff}}^{\text{pmm}} = 0.045 \text{ W m}^{-1} \text{ K}^{-1}$.

The effective diffusivity

The effective diffusivity is given in terms of the effective heat conduction, density and heat capacity as $\kappa_{\text{eff}} = k_{\text{eff}}/(\rho c)_{\text{eff}}$. Using the above approximations gives the results in Table 3. The value of $1 \text{ cm}^2 \text{ hr}^{-1}$ found from the experimental simulation agrees with these theoretical calculations and hence is reasonable.

Approximation	Diffusivity κ_{eff}
Parallel (lower bound)	$1.55 \times 10^{-8} \text{ m}^2 \text{ s}^{-1} = 0.56 \text{ cm}^2 \text{ hr}^{-1}$
Maxwell (lower bound)	$2.22 \times 10^{-8} \text{ m}^2 \text{ s}^{-1} = 0.80 \text{ cm}^2 \text{ hr}^{-1}$
Perrins	$2.27 \times 10^{-8} \text{ m}^2 \text{ s}^{-1} = 0.82 \text{ cm}^2 \text{ hr}^{-1}$
Numerical simulation	$2.77 \times 10^{-8} \text{ m}^2 \text{ s}^{-1} = 1.00 \text{ cm}^2 \text{ hr}^{-1}$
Cheng Torquato	$3.30 \times 10^{-8} \text{ m}^2 \text{ s}^{-1} = 1.19 \text{ cm}^2 \text{ hr}^{-1}$
Series (upper bound)	$1.34 \times 10^{-7} \text{ m}^2 \text{ s}^{-1} = 4.82 \text{ cm}^2 \text{ hr}^{-1}$

Table 3: The effective diffusivity in the various approximations and numerical simulation.

2.2.4 Obtaining κ_{eff} from experiments

Due to the rapidity of heat flow through a single bottle (Section 2.1) relative to an array of bottles, it is appropriate to use the diffusion equation with some experimentally measured effective diffusivity κ_{eff} . In the event that an experimentally derived value for κ_{eff} is required, the following will be of use. A solution of the 1D diffusion equation with oscillatory heating (such as diurnal heating) on one side is

$$T(x, t) = T_{\text{mean}} + A \exp\left(-\sqrt{\frac{\omega}{2\kappa_{\text{eff}}}}x\right) \sin\left(\omega t - \sqrt{\frac{\omega}{2\kappa_{\text{eff}}}}x\right). \quad (18)$$

This solution has the following properties:

- At $x = 0$, the temperature is sinusoidal with frequency ω and amplitude ($T(x = 0, t) = T_{\text{mean}} + A \sin \omega t$). This situation is often encountered with diurnal heating of pallets or containers by the sun either in transit or storage.
- The temperature of the interior ($x > 0$) is also sinusoidal with the same frequency ω , but there is a phase lag given by $\sqrt{\omega/2\kappa_{\text{eff}}}x$. This observation provides one method of measuring κ_{eff} .
- The amplitude of the internal temperature oscillations decays exponentially via the prefactor $\exp(-\sqrt{\omega/2\kappa_{\text{eff}}}x)$. This provides another method of measuring κ_{eff} .

2.3 Slowing temperature increases

In practical applications convective or mechanical mixing of the air surrounding packaged bottles would increase the speed of the heat transfer substantially. The value given in equation (2.2.2) should be considered as a ‘best practice’ value to be aimed for by wine distributors or storers. Values inferred from the literature, although never measured particularly carefully, are around $10 \text{ cm}^2 \text{ hr}^{-1}$ or more [4]. This is clearly an area of research that needs further experimental work. The determination of the effective diffusivity is a relatively straightforward experiment to perform using thermocouples and data loggers.

By reducing air flow around the bottles substantial slowing of the heat transfer can be obtained. Because κ_{eff} can theoretically be made small (an order of magnitude smaller than some experiments suggest) a study into the most effective use of thermal blankets, or even simple bubble-wrapping during transport is recommended. Theoretically, over the course of a couple of days in transit, only the bottles closest to the heat source are being overly heated. This suggests that using a thermal blanket or equivalent to reflect heat, reduce convection and to act as a sacrificial heat sink may ameliorate many potential overheating problems for short haul transport (2 days or less). For long haul transport (4 days or more) the entire container will reach close to the ambient temperature. In this scenario temperature controlled transport and storage is recommended.

2.4 Conclusion

Wine temperature was quantified using numerical simulation for two simple cases: an initially cool bottle standing in a hot environment; an initially cool, large pallet of bottles standing in a hot environment. These are the two extremes which can occur during the transportation and storage of wine. The results imply the following general conclusions.

1. A single bottle of wine exposed to raised ambient temperatures will achieve that ambient temperature in approximately one to two hours. This time is decreased if there is mixing of the wine such as induced by convection or mechanical agitation during transportation.
2. In contrast, if convection of air around wine bottles, cartons and pallets can be minimised, the interior bottles in a standard 12-bottle carton takes approximately four days to achieve ambient temperature. This is because the air, which is conducting the heat, has such a low thermal mass compared to the wine. This scenario can be thought of as ‘best practice’.
3. To achieve close to best practice, convection can be minimised with simple procedures such as shrink/bubble-wrapping pallets, or by using a thick thermal blanket to act as a sacrificial thermal buffer to protect the outer bottles (which achieve ambient temperatures within about a day).
4. The mathematical results also allow other scenarios to be investigated and quantified easily.

3 Gas transport through the cork

When the temperature in the bottle increases the pressure of the air between the wine and the cork increases, forcing air through the cork. As the bottle cools the reverse occurs, drawing fresh air into the bottle. This phenomena is known as cork breathing. We consider here the temperature induced pressure increase in the air gap, the volumetric expansion of the wine, and the permeability of the cork, deriving exact and approximate equations for the air flow through the cork.

3.1 Flow calculations

The increase in volume of the wine is proportional to temperature increase of the wine and is effected little by the pressure of the air

$$V_w(t) = V_w(0)(1 + \alpha_v(T_w(t) - T_w(0))), \quad (19)$$

where $V_w(t)$ [m³] is the volume of the wine, $T_w(t)$ [K] is the wine temperature at time t [s], and α_v [m³ K⁻¹] is the volumetric expansion coefficient of wine. The volume of the bottle, V_b , remains effectively constant hence the air volume, $V_a(t)$ [m³], is related to the wine volume by

$$V_a(t) + V_w(t) = V_b. \quad (20)$$

The flow of air through the cork is relatively slow and pressure driven, hence is well modelled by Darcy’s law

$$w(t) = k \frac{P(t) - P_0}{L}, \quad (21)$$

where $w(t)$ [m s⁻¹] is the air velocity through the cork, $k(t)$ is the permeability of the cork [m² s⁻¹ Pa⁻¹] (including the viscosity), $P(t)$ [Pa] is the pressure, P_0 is atmospheric pressure, and L [m] is the length of the cork. This flux of air through the cork is related to the loss of air mass through the cork by

$$\frac{dm_a(t)}{dt} = -\rho_a(t)w(t)A = -kA \frac{\rho_a(t)(P(t) - P_0)}{L}, \quad (22)$$

where $m_a(t)$ [kg] is the mass of air in the gap between cork and wine, $\rho_a(t)$ [kg m^{-3}] is the density of the air, and A [m^2] is the cross-sectional area of the cork.

The permeability, k , is in reality a function of time, although this time dependence only affects the flow minimally. When moist air is flowing out of the bottle, the viscosity will be higher and hence the permeability lower. When dry air flows into the bottle through the cork the permeability is higher. The level of moisture in the air is also temperature dependent. This may be a minor effect but one that can be easily considered by having k as a function of time in the governing equations.

The pressure in the air is modelled by the perfect gas law

$$\frac{P(t)V_a(t)}{m_a(t)T_a(t)} = \frac{P(0)V_a(0)}{m_a(0)T_a(0)} = \beta, \quad (23)$$

where $T_a(t)$ is the temperature of the air and β is a constant.

Combining (22) and (23) gives

$$\frac{dm_a(t)}{dt} = -\frac{k(t)A}{L} \left[\frac{\beta m_a^2(t)T_a(t)}{V_a^2(t)} - \frac{P_0 m_a(t)}{V_a(t)} \right], \quad (24)$$

with the volume correction, equations (19) and (20), giving $V_a(t)$.

Equation (24) is a logistic equation, common in population modelling, with slowly varying parameters; that is $m' = -c_1 m^2 + c_2 m$ with $c_1(t)$ and $c_2(t)$ slowly changing. The equilibrium for (24) occurs when

$$m_a = m_a(0) \frac{V_a(t)}{V_a(0)} \frac{T_a(0)}{T_a(t)} \equiv g(t), \quad (25)$$

hence as the temperature changes, driving volume and pressure changes, the differential equation (24) works to bring $m_a(t)$ into this balance. However, as $g(t)$ varies slowly with time, the mass of air is always chasing this equilibrium, $m_a \rightarrow g$, being closer to it if the cork permeability is large. Numerical solutions to (24) can easily be found and approximate and analytic solutions can also be found. These are explored in Section 3.3.

3.2 Limit of very permeable cork

If the cork closure is assumed very permeable (such as in the case of a defective cork), then the pressure responds rapidly to reach it's equilibrium state, shown in equation (25). The volumetric expansion of wine with an expansion coefficient of $\alpha_v = 2 \times 10^{-4} \text{ K}^{-1}$, gives an approximate increase in wine volume of 4.5 ml over 30 degrees. This is comparable to the head space volume of 5-15 ml. Anecdotally, this is thought to be cause of corks being expelled from the bottle during long term transport when the head space is too small. Thus volumetric wine expansion can cause air loss through the cork of the order of 30 % to 100%.

The mass of air in the head space will also change due to the air expansion and loss through the cork. If $dT_a = T_a(t) - T_a(0)$ then the relative change in mass, assuming no wine expansion, is

$$\frac{m - m_0}{m_0} = \frac{V_a(0)T_a(0)}{V_a(0)T_a(t)} - 1 = \frac{1}{1 + dT_a/T_a(0)} - 1 \quad (26)$$

$$\approx \left(1 - \frac{dT_a}{T_a(0)} \right) - 1 \approx -\frac{dT_a}{T_a(0)}. \quad (27)$$

This gives an approximate measure of the air mass change due to air pressure changes. For a temperature rise of 30 degrees, an initial temperature of $T_a(0) = 283$ K (10° C) this gives magnitudes of approximately 11% mass flow. This is an upper bound on the air flow into the bottle of approximately 11% mass loss/gain in the course of a 30 degree temperature rise during one day. Hence approximately ten days of diurnal temperature changes will change virtually all the air in the bottle in the limit of a very permeable cork due to air expansion changes only.

3.3 Approximate solutions

This section explores some approximate solutions to equation (24) with the cork no longer very permeable so that its permeability is now important. Each of the solutions assume that the driving temperature, $T(t)$, changes slowly or remains close to the initial equilibrium state. It is not immediately apparent which approximation is the most valid until numerical simulations can compare the results with the full numerical solution. In our simulations we consider no volumetric wine expansion, equivalent to the situation of a large head space. Later work will consider the effect of air loss due to both wine expansion and air temperature.

It is informative here to non-dimensionalise the system with respect to typical scales:

$$m_a(t) = m_a(0) m(t^*), \quad V_a(t) = V_a(0) V(t^*), \quad (28)$$

$$P_a(t) = P_a(0) P(t^*), \quad t = t_0 t^*, \quad (29)$$

$$k(t) = k(0) k^*(t^*), \quad (30)$$

where $*$ denotes non-dimensional variables, and the typical time scale t_0 can be shown to be

$$t_0 = \frac{L V_a(0)}{k(0) A P_a(0)}.$$

Using these scalings (24) reduces to

$$\frac{dm(t)}{dt} = -c_1(t) m(t)^2 + c_2(t) m(t), \quad (31)$$

where we have dropped the $*$ notation herein, and

$$c_1(t) = \frac{k(t) T(t)}{V^2(t)}, \quad c_2(t) = \frac{k(t)}{V(t)}. \quad (32)$$

Changes in the temperature $T(t)$ forces equation (31) from the equilibrium state, $m = c_2(t)/c_1(t) = V(t)/T(t) = \gamma(t)$, with $k(t)$ and $V(t)$ changing slightly. We note that $c_1(t)$ contains the main time dependent term $T(t)$, which drives the process. However, $c_2(t)$ only varies slightly with time, as both k and V only change slightly with temperature and time.

First Approximate Solution

The first approximate solution assumes $c_1(t)$ and $c_2(t)$ are approximately constant in equation (31), leading to

$$m(t) \approx \frac{\gamma m(0)}{m(0) + (\gamma - m(0))e^{-c_2 t}}, \quad (33)$$

where $\gamma \equiv \gamma(t)$ and $c_2 \equiv c_2(t)$. This solution will be exact if γ and c_2 are constant. As $t \rightarrow \infty$ this gives the equilibrium solution $m \rightarrow \gamma$. This solution is most valid when the temperature change is a rapid jump, giving new values of c_1 and c_2 which do not then change with time.

Second Approximate Solution

A second approximate solution uses a technique described in [10]. The method uses two different time scales, $t_0 \equiv t$ and $t_1 \equiv \epsilon t$, with ϵ small and $c_2 = c_2(t_1)$ and $\gamma = \gamma(t_1)$. That is, c_1 and c_2 vary on the slower time scale, while $m(t)$ chases the equilibrium on a faster time scale. The mass is written as $m = m(t_0, t_1, \epsilon)$ with equation (31) becoming

$$\frac{\partial m}{\partial t_0} + \epsilon \frac{\partial m}{\partial t_1} = -c_2(t_1)(m - \gamma(t_1)). \quad (34)$$

Expanding in a perturbation series $m = m_0(t_0, t_1) + \epsilon m_1(t_0, t_1) + \dots$ and equating coefficients gives

$$\frac{\partial m_0}{\partial t_0} = -c_2(t_1)(m_0 - \gamma(t_1)) \quad \text{and} \quad \frac{\partial m_1}{\partial t_0} = -c_2(t_1)m_1 - \frac{\partial m_0}{\partial t_1}. \quad (35)$$

These two equations have solutions, using the initial condition $m = m_a(0) + \epsilon 0 + \dots$,

$$m_0 = (m(0) - \gamma)e^{-c_2 t_0} + \gamma, \quad (36)$$

$$m_1 = \left(\gamma' t + \frac{1}{2}(m(0) - \gamma)c_2' t^2 - \frac{\gamma'}{c_2} e^{c_2 t} + \frac{\gamma'}{c_2} \right) e^{-c_2 t_0}, \quad (37)$$

where γ and c_2 are functions of t_1 and hence $\gamma' = d\gamma/dt_1$. This solution satisfies the initial condition $m = m(0)$ and has the long term behaviour

$$m(t) \approx \gamma(\epsilon t) - \epsilon \frac{\gamma'(\epsilon t)}{c_2(\epsilon t)}. \quad (38)$$

That is, the mass attempts to reach the equilibrium point γ but since this equilibrium keeps changing slowly with time, it lags by a small amount.

Third Approximate Solution

Our third approximate solution is to assume $c_1(t)$ is a slowly varying function of time and that $c_2(t) = c_2$ remains constant, since only c_1 contains the driving term $T(t)$ and c_2 contains terms which only vary slightly with time. With this assumption the solutions obtained in [10] can be followed exactly to give

$$m \approx \frac{\gamma(\epsilon t)m(0)}{m(0) + \left(\gamma(\epsilon t) - \frac{\gamma(\epsilon t)}{\gamma(0)}m(0) \right) e^{-c_2 t}} - \epsilon \frac{\gamma'(\epsilon t)\gamma^2(0) - \gamma'(0)\gamma^2(\epsilon t)e^{-c_2 t}}{c_2\gamma^2(0) \left(1 + \left[\frac{1}{m(0)} - \frac{1}{\gamma(0)} \right] \gamma(\epsilon t)e^{-c_2 t} \right)^2}. \quad (39)$$

This has the required behaviour that at $t = 0$ then $m(0) = 0$. As $t \rightarrow \infty$ then $m \rightarrow \gamma - \epsilon \frac{\gamma'}{c_2}$ indicating the same time lag behaviour as shown earlier. Usually the temperature change is gradual, moving the system from an initial equilibrium state when $m(0) = \gamma(0) = 1$ towards a new equilibrium state as $\gamma(t)$ and $c_2(t)$ change with temperature. If this were the case the solution is greatly simplified to be (38). However, if there is an initially rapid rise in temperature then the initial state can be considered not to be in equilibrium, so $m(0) = 1$ but $\gamma(0) \neq 1$, and (39) is necessary. Note that the first term in (39) is similar, but not exactly the same as (33).

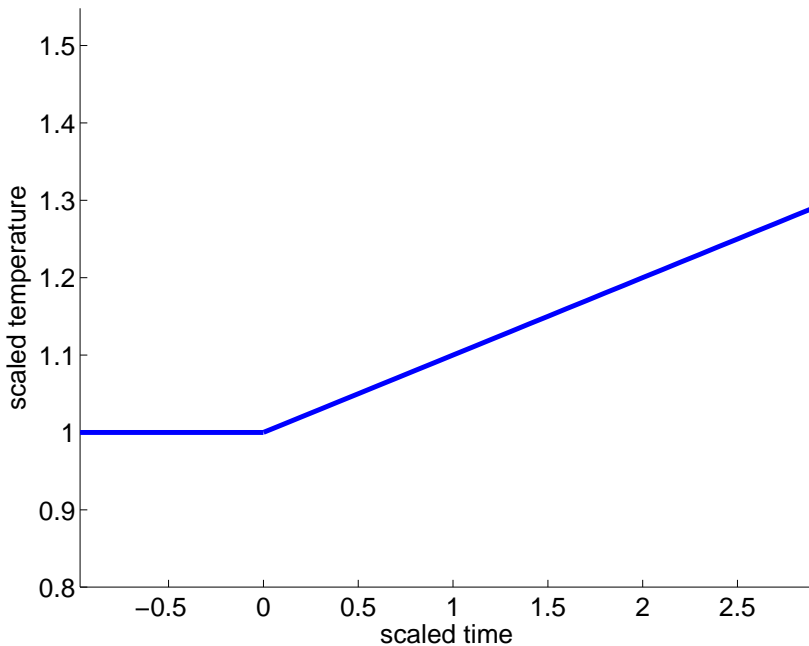


Figure 7: The temperature change being considered, a gradual linear increase.

3.4 Results

This section considers the numerical and approximate solutions for two different temperature change cases. The first case is a gradual rise in temperature (see Figure 7) and the second case a sinusoidally variable temperature for different amplitude and period.

Figure 8 shows the mass of air changing as a function of time when the temperature changes linearly as $T = 1 + \epsilon t$, $\epsilon = 0.1$ (as shown in Figure 7) with $V(t) = k(t) = 1$, and $m(0) = 1$. Equation (39) represents the full numerical solution slightly better than (37). The asymptotic solution given by (38) is also shown. As discussed earlier, the mass of air approaches this asymptotic solution for large time, mirroring the lower equilibrium solution $\gamma(t)$ but with a lag $\epsilon \gamma'(\epsilon t)/c_2(\epsilon t)$. Approximations one (33) and approximation two (zeroth order, (36)) both asymptote to the wrong solution $\gamma(t)$, although they well represent the exact solution for small time. All solutions remain sandwiched between the lower limit, $m = \gamma(t)$, and the upper limit, equation (38).

Of main interest for the wine transport and storage is regular diurnal temperature changes and a calculation of the mean air flow in and out of the cork. That is, for a temperature profile

$$T = 1 + a \sin(\epsilon t). \quad (40)$$

Figure 9 shows the air mass change for a sinusoidal temperature change $T = 1 + 0.1 \sin(\epsilon t)$ with $\epsilon = 0.3$. The same notation is used as for Figure 8. Many of the curves are indistinguishable except at small times. Approximations (39) and (37) almost perfectly match the asymptotic solution given by equation (38). The inaccurate approximation (36) matches the highly permeable cork case $m = \gamma(t)$. For this large value of ϵ the numerical solution does not match the various asymptotic solutions. For $\epsilon < 0.1$ the numerical result matches the asymptotic

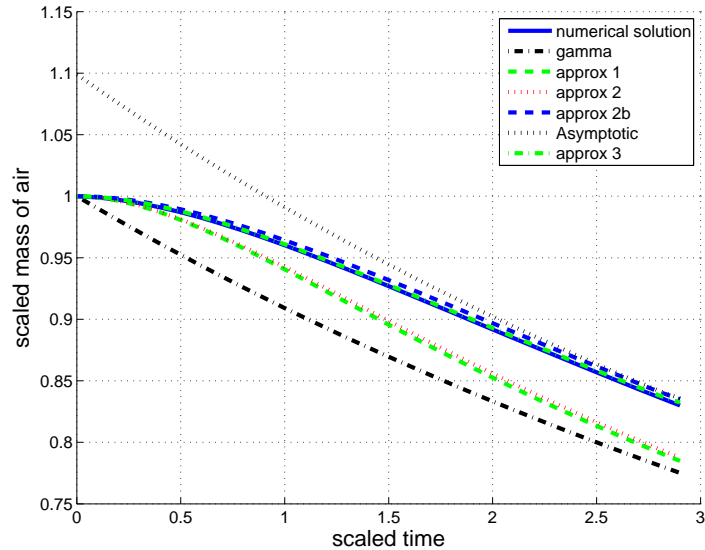


Figure 8: Air mass versus time for a linear temperature rise. Blue solid line is numerical solution to (24). Black dot-dash line is $m = \gamma(t)$. The green dashed line is approximation one (33). The red dotted line the second approximation (36). The full second approximation, (36) and (37), is the blue dashed line ‘approx 2b’. The third approximation, (39), is the green dot-dash line. The asymptotic solution (38) is the upper black dotted line.

solution.

We require the difference between the maximum and minimum values of air mass, $\overline{m} = 2(\max(m) - \min(m))$, since this is how much air has flowed in and out of the bottle. Figure 10 illustrates \overline{m} for varying ϵ and a , showing an expected linear behaviour of mass flux with increasing magnitude, at least for small a . This illustrates the limitation of the various approximations as ϵ increases. When $\epsilon \rightarrow 0$ the temperature changes are so slow that in effect the cork is completely permeable. As ϵ increases, the oscillations in temperature are fast enough that the air does not have time to flow out of the cork before the temperature has reversed direction. Hence one expects that $\overline{m} \rightarrow 0$ as ϵ increases. This behaviour is not reflected in any asymptotic solutions as it is a highly nonlinear effect. Large ϵ corresponds to a long period of temperature oscillations such as seasonal variation under cellar conditions.

3.5 Future work

There are several aspects of this work that could be explored. First, the permeability of wine cork is not well known and this is the crucial parameter in determining mass of air flow through the cork. Some data exists on dry cork board ($k \approx 2.4 - 5.7 \times 10^{-11} \text{m}^2$ [7]) however this is not indicative of permeability of a wet compressed cork. Second, the numerical results on air flow through cork included here took $V(t) = k(t) = 1$ which is a simplification to allow each effect to be studied separately. Future work will include temperature dependent expansion of the wine, the viscosity of moist and dry air, and the temperature dependent moisture content in the air. An additional effect is the time delay between thermal diffusion into the air and wine within the bottle, the wine exhibiting a longer time lag. This may have

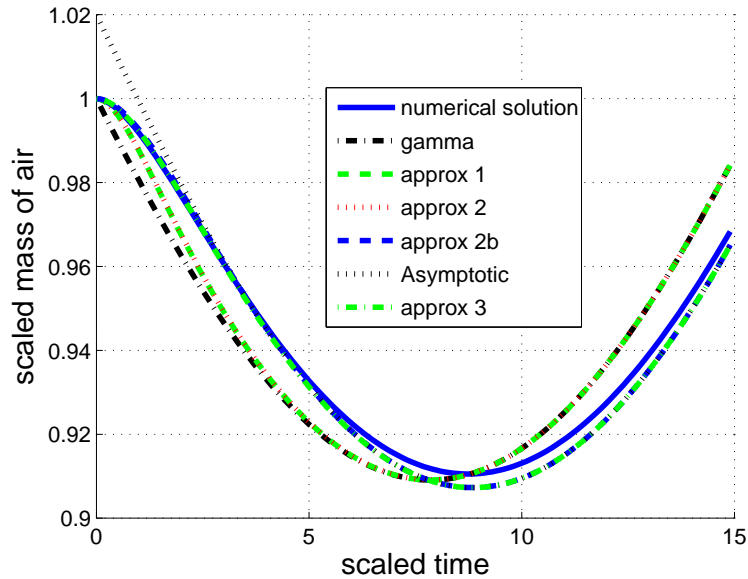


Figure 9: Air mass change for sinusoidal temperature variation with the same notation and parameters as Figure 8

a small effect on the air flow through the cork.

4 Oxidation of wine

Wine changes in the bottle through a sequence of oxidative reactions, mediated through the supply of oxygen to the wine. During storage at uniform temperature, oxygen is supplied to the wine by diffusion through the cork, and this occurs at a very slow rate. During transport, or if the external temperature fluctuates in storage, thermal expansion and contraction of the wine can cause forced flow of oxygen through the cork, and this is described by Darcy's law, as described in Section 3.

4.1 Wine chemistry

The primary oxidative reaction of importance is the oxidation of a class of phenols. Amongst these are the tannins, and the oxidative effect on some of these is to cause *browning* of the wine, for example discolouration [5]. A secondary effect of the oxidation of phenols is the production of hydrogen peroxide, H_2O_2 , and the peroxide is a strong oxidiser, which reacts with the alcohol (ethanol, $\text{C}_2\text{H}_6\text{O}$) to produce acetaldehyde, $\text{C}_2\text{H}_4\text{O}$, which causes deterioration in aroma and taste of the wine.

In order to prevent such reactions, it is common practice to add sulphur dioxide, SO_2 , which reacts directly in its molecular form with the peroxide to form sulphuric acid, H_2SO_4 . When dissolved in water, SO_2 dissociates to form the bisulphite ion HSO_3^- , and this bisulphite takes acetaldehyde out of solution by forming a bound complex. This dissociation of SO_2 is highly pH dependent.

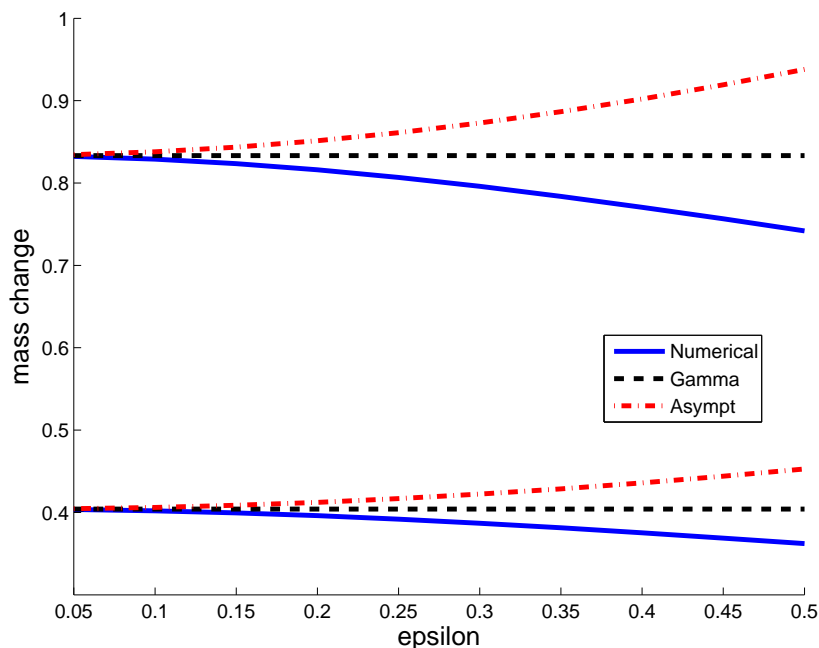
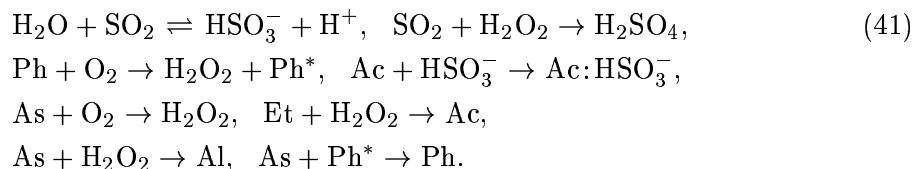


Figure 10: Total diurnal mass change versus parameters a and ϵ in equation (40). The curve shows mass flow versus ϵ with $a = 0.1$ (lower curves) and $a = 0.2$ (upper curves). The behaviour is shown using numerical solution (solid blue lines), the limiting solution $m(t) = \gamma(t)$ (black dashed lines), and asymptotic solution (equation (38), red dot-dash lines).

Sometimes ascorbic acid (vitamin C, $C_6H_8O_6$) is added to prevent discolouration; it does this by effectively reversing the phenol oxidation. However, ascorbic acid has other undesirable effects: it reacts with peroxide to form an aldehyde, another chemical which causes taste deterioration, and it oxidises to form more peroxide.

4.2 Differential equations

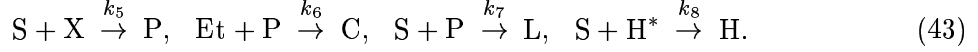
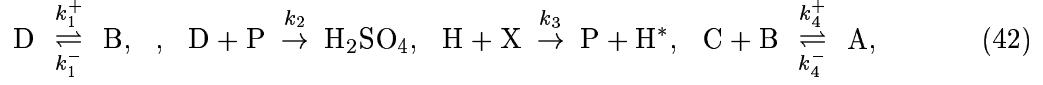
A set of reactions to describe these processes is the following:



In these reactions, we denote ascorbic acid as As, ethanol as Et, acetaldehyde as Ac, aldehyde as Al, phenol as Ph or Ph^* ; Ph^* represents the more oxidised, discoloured form. The bound acetaldehyde–bisulphite complex is denoted $Ac:HSO_3^-$.

We rewrite these equations using the abbreviations D for dioxide, B for bisulphite, P for peroxide, H and H^* for the phenol and oxidised phenol, X for oxygen, C for acetaldehyde, S for ascorbic acid, A for the $Ac:HSO_3^-$ complex, and L for the aldehyde. Adding rate constants,

they are



We apply the law of mass action to these reactions, and this leads to the following set of ordinary differential equations, in which we use the same symbols to denote the concentrations of the chemicals. We suppose the wine is well-mixed, which will be a valid assumption during transport, although not necessarily during storage, and we also suppose that ethanol is essentially unchanged, being present in large quantity (e. g., 12% by volume). The equations are

$$\begin{aligned} \dot{D} &= k_1^- B - k_1^+ D - k_2 DP, \\ \dot{B} &= -k_1^- B + k_1^+ D - k_4^+ BC + k_4^- A, \\ \dot{P} &= k_3 HX + k_5 SX - k_6 P - k_7 SP - k_2 PD, \\ \dot{H} &= -k_3 HX + k_8 SH^*, \\ \dot{H}^* &= k_3 HX - k_8 SH^* [-R], \\ \dot{X} &= -k_3 HX - k_5 SX [+V], \\ \dot{C} &= -k_4^+ BC + k_4^- A + k_6 P, \\ \dot{S} &= -k_5 SX - k_7 PS - k_8 SH^*, \\ \dot{L} &= k_7 PS \\ \dot{A} &= k_4^+ BC - k_4^- A \end{aligned} \quad (44)$$

where the overdot represents the time derivative.

The posited terms V and R warrant some discussion. As wine matures, the phenols are oxidised to form larger molecules, and these eventually precipitate and fall out of solution. If necessary, this could be described by a suitable loss term R . Consulting equation (44), we see that oxygen is depleted by its reaction, principally with the phenols, and this depletion takes about a week under normal circumstances [1]. Once the oxygen is removed, there is no source for peroxide, total SO_2 ($B + D + A$) is conserved, the reactants reach steady state, and the reactions cease. Thus the continuing maturation and aging of wine requires the supply of oxygen, and this is indicated by the source term V .

4.3 Determining a usable model

In order to analyse these equations, we would need estimates of the rate constants and, importantly, their variation with temperature. However, this information is not readily available and is unlikely to be available in the future. Instead, we are motivated by the experimental results of [8], who interpreted SO_2 loss and browning in terms of a first order rate equation. Implicitly, he supposes that SO_2 satisfies a first order rate equation of the form

$$\dot{D} = -k_{\text{eff}} D, \quad (45)$$

where the effective rate coefficient k_{eff} is a strong function of temperature of the Arrhenius form

$$k_{\text{eff}} = k_0 \exp \left[-\frac{E}{RT} \right], \quad (46)$$

where E is the activation energy, R is the gas constant, and T is absolute temperature. One object of analysing the system of equations (44) is to see in what circumstances an effective equation of the form (45) can be obtained. In the present paper, we limit ourselves to this goal.

We suppose that the dissociation reactions are fast. If $k_4^\pm \gg \frac{1}{TS}$, where TS is the time scale of interest (of SO_2 decay), then $k_4^- A \approx k_4^+ BC$ determines A . If also $k_1^\pm \gg \frac{1}{TS}$, then $k_1^- B \approx k_1^+ D$ and thus the dioxide satisfies the rate equation

$$\dot{D} \approx -k_2 PD. \quad (47)$$

This provides a single rate equation for D , providing the peroxide concentration is constant. It remains to consider whether this is true.

We will suppose that the peroxide reactions are fast, since peroxide is a strong oxidant, so that we take the equation for \dot{S} in (44) to be at equilibrium. Then

$$P \approx \frac{k_3 H X + k_5 S X}{k_6 + k_7 + k_2 D}. \quad (48)$$

We suppose also that (with a source term V) the oxygen equation in (44) is fast (since oxygen concentrations are very low), so that X equilibrates as

$$X \approx \frac{V}{k_3 H + k_5 S}. \quad (49)$$

Then (47) becomes

$$\dot{D} = -\frac{k_2 V D}{k_6 + k_7 S + k_2 D}. \quad (50)$$

The rate law (50) forms the essential conclusion of this analysis. Further forms are possible, depending on the behaviour of the ascorbic acid S . If the removal of S is fast, then $S \approx 0$, or if the reaction is slow, then $S \approx \text{constant}$. In any event, (50) takes the well known Michaelis-Menten form

$$\dot{D} = -\frac{VD}{K + D}, \quad \text{where } K = \frac{k_6 + k_7 S}{k_2}. \quad (51)$$

In this form there are good prospects to be able to fit this model to experimental results and obtain a useful model of the aging process. There are only 3 parameters (k_2 , k_6 and k_7) to fit experimental data to. The limited experimental data available on the aging process supports the Michaelis-Menten form for the model and in some cases suggests an even simpler first order form with a single rate constant that is temperature dependent through an Arrhenius relationship. It is a relatively straightforward experiment to perform to test whether the single Arrhenius rate constant is applicable. Details of this experiment can be found in [8]. If $D \ll K$, then we regain the first order rate equation (45). If, for example, $S = 0$ or k_7 is small, then, with an obvious notation,

$$k_{\text{eff}} = \frac{k_2 V}{k_6} = \frac{k_2^0 V}{k_6^0} \exp \left[-\frac{(E_2 - E_6)}{RT} \right], \quad (52)$$

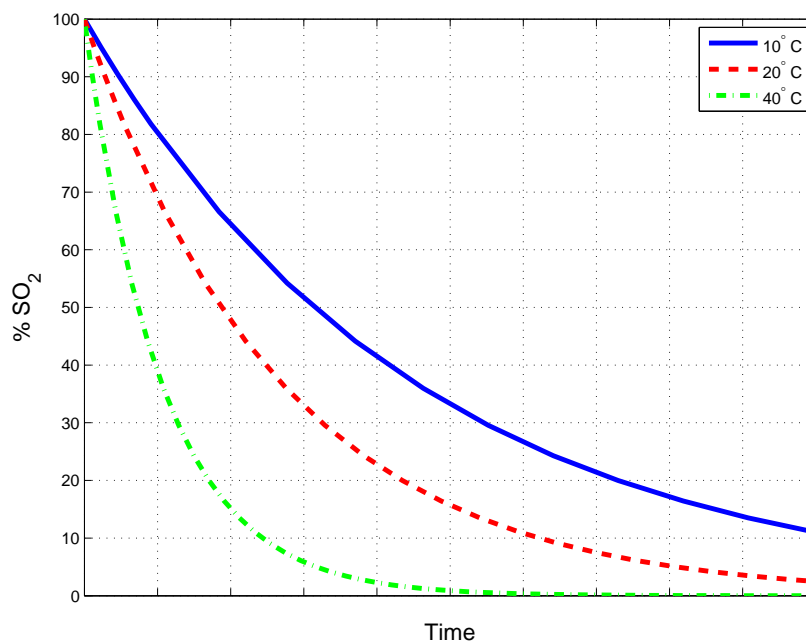


Figure 11: Percentage decline in SO_2 for 3 different temperatures from solving (45) using the data from [8].

and the effective activation energy of the reaction is $E = E_2 - E_6$.

As a first point in determining an appropriate model for the aging process experimental data should be fitted to (45). If this provides a good fit then a more complicated model is not required. If the fit is not good then the the Michaelis–Menten form (50) should be used.

4.4 Applying a model

Using the limited data available in the literature for one red wine type (see [8]), calculations were performed for the first order Arrhenius case (45) to quantify the effect of elevated temperature on the SO_2 reduction and the browning. From [8, 1] the activation energy for the red wine the used in their experiments was $E = 35,700 \text{ kJ mole}^{-1}$ for SO_2 and $E = 66,400 \text{ kJ mole}^{-1}$ for browning. Figure 11 shows the results of solving (45) for the SO_2 . The percentage decline in SO_2 is shown for 3 different temperatures (10, 20 and 40°C) versus time. Clearly the elevated temperatures have a dramatic effect on the SO_2 decline with the higher temperatures leading to more rapid SO_2 reduction.

Results of solving (45) were compared to ideal cellaring conditions at 10°C and expressed as a percentage of time to reach the same state (% of SO_2 present or % of browning occurring) relative to ideal conditions. Figure 12 shows the effect of elevated temperature on the shelf life. At 20°C the time to reach the critical SO_2 level was 59% of ideal conditions and 38% for browning. That is the shelf life measured by SO_2 level is almost half and measured by browning is approximately one third compared to ideal cellar conditions. This dropped dramatically for 40°C to 23% and 8% respectively. Depending on which is the critical parameter (SO_2 level or browning) this means that at 40°C the shelf life is between 8% and 23% of the

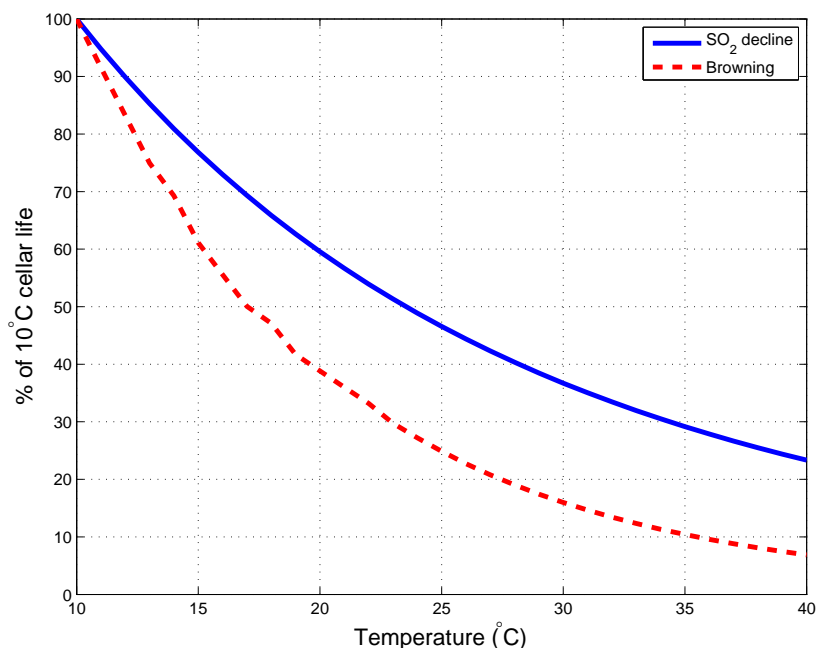


Figure 12: The temperature dependence of shelf life of the red wine considered in [8] as a percentage of the shelf life at ideal cellaring conditions

ideal cellaring shelf life. So, for example, a wine with a shelf life of approximately 10 years under ideal conditions would have its shelf life reduced to between about 10 months and 2.3 years depending on which measure of shelf life (browning or SO₂ level) was considered.

With better data derived from experimental work this method could be used to give reasonable estimates for the reduction in shelf life of wine when subjected to elevated temperatures. Both Michaelis-Menton type reactions and first order reactions can be considered in a straightforward manner in these types of models. Different wines will no doubt have different activation energies and these will need to be determined experimentally for each wine type to use these models. It is a relatively straightforward experiment to determine these activation energies and this is certainly the first step that should be considered to determine useful data for the models.

5 Conclusion

In summary three separate models have been developed for various aspects related to the shelf life of wine. These are heating of wine during transport, oxygen ingress through the cork and oxidative chemistry models. Estimates for the time wine takes to almost reach ambient external temperature for both single bottles (order of two hours) and in a container (order of 4 days) have been obtained. Long haul transport was found to be the area most affected by heating issues. Air flow through the cork was determined under oscillatory temperature regimes (either a domestic diurnal scenario or a longer cellaring seasonal one). A critical parameter is the cork permeability which is currently unavailable for wet compressed cork

as found in the bottle. It is recommended that straightforward experiments be conducted to determine this parameter. The model developed for the oxidation of wine was shown to reduce down to the well known Michaelis-Menton form or the even simpler first order Arrhenius form under certain assumptions. If these relationships are appropriate then relatively simple models of the shelf life of components (for example sulphur dioxide or browning) are easily developed. Experiments to test the model assumptions have been recommended.

Followup from the industry partner (Provisor) and wine producing companies at an industry forum shows that there is considerable interest in this project. The heating of wine in containers during long haul transport is of particular concern to the major exporting wineries as they sometime suffer substantial losses as overheating occurs in shipping to the Northern hemisphere due to transitting through the tropics. Many companies have thermocouple traces (all unpublished data) of temperature within the containers that they have difficulty interpreting. The current study will be of assistance to them and this is an area of future research. Oxygen ingress through the cork is considered less of an issue as increasingly wine is being bottled with other closures (mostly screw cap) although it is important in some markets (notably the USA and France) where cork is still the preferred closure. The models for the oxidation of wine presented is an area of ongoing research in conjunction with Provisor. Future work will be to construct similar models for reductive chemistry which is more applicable to wine bottled under screw cap. Other components of the wine, such as tannins and flavours, will also be included in the models.

References

- [1] Boulton, R.B., Singleton, V.L., Bisson, L.F. & Kunkee, R.E. (1997) *Principles and practices of winemaking*, CBS, New Delhi, India.
- [2] Cheng, H. & Torquato, S. (1997) Effective conductivity of dispersions of spheres with a superconducting interface, *Proc. Roy. Soc. London A*, **453**, 145-161.
- [3] Kaye, G.W.C. & Laby, T.H. (1973) *Table of physical and chemical constants and some mathematical functions*, Longman, New York.
- [4] Laffer, P.L. (2004) Management of wine quality during transport, *Proc. twelfth Australian wine industry technical conference*, Ed. R. Blair, P. Williams and S. Pretorius, 219-221.
- [5] Li, H., Guo, A. & Wang, H. (2008) Mechanisms of oxidative browning of wine, *Food Chem.* **108**, 1-13.
- [6] Maxwell, J.C. (1891) *A treatise on electricity and magnetism*, Dover, New York.
- [7] Nield, D.A. & Bejan, A. (1999) *Convection in porous media*, Springer, New York.
- [8] Ough, C.S. (1985) Some effects of temperature and SO₂ on wine during simulated transport or storage, *Amer. J. Enol. Vitic.* , **36** (1), 18-22.
- [9] Perrins, W.T., McKenzie, D.R. & McPhedran, R.C. (1979) Transport properties of regular arrays of cylinders. *Proc. Roy. Soc. London, Ser. A*, **369**, 207-225.
- [10] Shepherd, J.J. & Stojkov, L. (2007) The logistic population model with slowly varying carrying capacity, *ANZIAM J(E)* **47**, C492-C506.